NACA RM E53I14

RESEARCH MEMORANDUM

EVAPORATION AND SPREADING OF ISOOCTANE SPRAYS IN HIGH-VELOCITY AIR STREAMS

By Donald W. Bahr

Lewis Flight Propulsion Laboratory
Cleveland, Ohio

NATIONAL ADVISORY COMMITTEE
FOR AERONAUTICS

WASHINGTON

November 16, 1953

NATIONAL ADVISORY COMMITTEE FOR AERONAUTICS

RESEARCH MEMORANDUM

EVAPORATION AND SPREADING OF ISOOCTANE SPRAYS IN HIGH-VELOCITY AIR STREAMS

By Donald W. Bahr

SUMMARY

The evaporation and spreading of isooctane sprays were investigated over a range of inlet-air conditions common in ram-jet engines. Isooctane was injected contrastream from a simple-orifice fuel injector into air flowing through an 8-inch-diameter duct. The total and the liquid fuel distribution across the duct were determined.

The distribution profiles were measured over the following ranges of variables: inlet-air temperatures, 540° to 850° R; inlet-air velocities, 100 to 350 feet per second; inlet-air static pressures, 18 to 35 inches of mercury absolute; fuel-injection pressure drops, 25 to 85 pounds per square inch; diameters of fuel injector orifice, 0.024 to 0.041 inch; and axial distances from fuel injector, 5 to 18 inches. Over these ranges, expressions were obtained which related the evaporation rate and the degree of spreading of the sprays to the experimental variables.

INTRODUCTION

The two primary considerations in the preparation of fuel-air mixtures in ram-jet and afterburner combustors are the evaporation rate and the distribution pattern of the fuel spray. The location of the fuel injectors relative to the flame holders, for optimum combustor performance, is dependent on these two factors. This report describes an experimental investigation of the effect of combustor-inlet conditions on the evaporation and spreading of a gasoline-type fuel injected contrastream from a simple orifice; the investigation was conducted at the NACA Lewis laboratory.

The evaporation rate of fuel sprays in high-velocity air streams has been investigated analytically (ref. 1). The results of an experimental study, in which rather limited ranges of air-flow conditions were utilized, are reported in reference 2. In reference 3, a theoretical and experimental treatment of fuel-spray spreading in high-velocity air streams is described; however, only sprays consisting of either a highly volatile or a nonvolatile fuel were considered.

The object of this study was to relate the evaporation and spreading rate of isooctane sprays to inlet-air and fuel-injection parameters common to ram-jet engines and afterburners. Isooctane was injected contrastream into air flowing through a duct 8 inches in diameter. Samples of the spray were withdrawn with a probe downstream of the simple-orifice fuel injector. Both the total fuel and the liquid fuel distribution across the duct were determined by sampling techniques described in reference 3. The measurements were made over ranges of inlet-air temperatures, inlet-air velocities, inlet-air static pressures, fuel-injection pressures, fuel orifice diameters, and axial distances from the fuel injector.

SYMBOLS

The following symbols are used in this report:

D	diameter of fuel-injector orifice, in.
exp	exponential, [$\exp(x) = e^x$]
f	fuel-air ratio
L	axial distance from fuel injector, in.
M	index of fuel-spray spreading, sq ft
N	spray evaporation, percent
p_a	air pressure, in. Hg abs
p_f	fuel-injection pressure drop, lb/sq in.
R	radius of duct, ft
r	radial distance from spray axis, ft
T_a	inlet-air temperature, $^{\circ}R$
V_a	inlet-air velocity, ft/sec
W_a	air-flow rate, lb/sec

Subscripts:

l	liquid
o	over all
t	total

APPARATUS

Installation

A schematic diagram of the test installation is presented in figure 1. Air at 40 pounds per square inch gage was drawn from the laboratory air-supply system and exhausted into the altitude-exhaust system. The air flow was regulated upstream of the test unit by two butterfly valves: an 8-inch-diameter valve and, in a bypass line, a 4-inch-diameter valve. The ambient pressure in the test section was controlled downstream of the test unit by a similar system of two butterfly valves. The air was preheated by burning MIL-F-5624A grade JP-4 fuel with a small portion of the air in a turbojet-engine combustor.

Test section. - The preheated air passed through a 12-foot length of straight Inconel pipe having an outside diameter of $8\frac{5}{8}$ inches and a wall thickness of 1/8 inch. A monel wire cloth, 30 by 28 mesh of 0.013-inch-diameter wire, was placed in the duct $2\frac{3}{4}$ feet downstream of the preheater. The sampling station was located $6\frac{3}{4}$ feet downstream of the wire cloth, and fuel nozzles were positioned 5 to 18 inches upstream of the sampling station. Quench water was injected into the air stream downstream of the sampling station. The air then flowed through the expansion bellows to the downstream control valves and into the altitude-exhaust system.

Fuel and fuel system. - Isooctane, which met A.S.T.M. specifications, was used throughout the investigation as the fuel. This fuel was delivered to the fuel injector by nitrogen pressure. All the injectors investigated were constructed of 1/4-inch-diameter Inconel tubing with a 0.031-inch wall. A single orifice was drilled 1 inch from the sealed end of the tube and reamed to remove any burrs. Orifice diameters of 0.024, 0.033, and 0.041 inch were utilized, and the fuel-injector orifice in each case was positioned on the center line of the test section and pointed directly upstream.

Instrumentation

The air was metered by a variable orifice located upstream of the air-flow control valves. The orifice was preceded by a 12-foot straight length of pipe. The air temperature was measured with unshielded thermocouples at the orifice and at a distance of $3\frac{1}{2}$ feet upstream of the sampling station. Static-pressure taps were positioned at the thermocouple stations and at the sampling station.

The isooctane flow rate was determined with two calibrated rotameters. Measurements of the fuel temperature and pressure were taken at

the fuel injector. The JP-4 fuel was also metered by a calibrated rotameter, and its pressure was measured at the air preheater.

Sampling System

A schematic diagram of the sampling system is shown in figure 2. Samples of the spray were continuously withdrawn from the test section with a probe. The fuel-air sample flowed vertically downward into the analyzing section.

Probe. - The probe was constructed of 3/16-inch outside-diameter Inconel tubing with a 0.032-inch wall. The 2-inch section of the probe, which pointed directly into the air stream, was tapered to the probe mouth. Remote actuation of the probe was attained with a probe positioner with which a complete vertical traverse across the test section was possible.

Analyzing section. - The sample was conducted from the probe to an electric-resistance heater to ensure complete evaporation of the collected fuel. When necessary, diluent air was added to the sample at the inlet of the heater. The diluent-air flow rate was metered with a critical-flow orifice.

The flow rate of the heated sample gas was measured with a calibrated rotameter. The temperature and static pressure of the sample were determined at the rotameter inlet. From the rotameter, the sample was conducted through a control valve to a two-cylinder-diaphragm pump. The sample was then discharged from the pump to an NACA mixture analyzer (ref. 4). A continuous analysis of the sample was obtained, and the fuel-air ratio of the sample was indicated on a self-balancing potentiometer.

METHODS AND PROCEDURE

At a single air-flow setting and fuel-injection rate, both the total and the liquid fuel distribution across the test section were determined. The fuel temperature was held constant at approximately 80° F, and the profiles were measured over the following ranges of variables:

Inlet-air temperatures, °F	80 to 390
Inlet-air velocities, ft/sec	100 to 350
Inlet-air static pressures, in. Hg abs	18 to 35
Axial distances from fuel injector, in.	5 to 18
Fuel-injection pressure drops, lb/sq in.	25 to 85
Fuel-injector orifice diameters, in.	0.024 to 0.041

Sampling Methods

Two techniques of withdrawing the spray samples were employed:

(1) The sample was withdrawn at stream velocity. All the fuel-air mixture intercepted by the probe was collected, and the total fuel-air ratio at the sampling point was determined.

(2) The sample was withdrawn at a rate less than 40 percent of the stream velocity. Most of the intercepted flow was forced to spill around the probe. Almost all of the fuel droplets entered the probe because of their higher momentum; this is known as the spillover method (ref. 3) of determining the liquid fuel-air ratio at the sampling point.

The ratio of the weight of droplets collected to the weight that would be collected if no droplets were deflected around the probe is defined as the collection efficiency of the spillover method. A theoretical analysis of the collection efficiencies of cylinders, ribbons, and spheres is presented in reference 5. This study demonstrates that the collection efficiency is increased as the duct air velocity and the droplet diameter are increased and the probe size is decreased.

Although the configurations are not identical, the results of reference 5 may be applied to indicate qualitatively the collection efficiency of the probe used in this investigation. Based on this analysis, the following efficiencies are indicated at an air temperature of 80° F and an air static pressure of 25 inches of mercury absolute:

Diameter of isooctane droplets, microns	Collection efficiency, percent, at -	
	Duct air velocity of 150 ft/sec	Duct air velocity of 300 ft/sec
5	69	79
8	83	90
10	88	93
20	96	98

Complete spillover of the intercepted flow was assumed in the analysis of reference 5. In the spillover measurements of this investigation, however, about 40 percent of the intercepted flow was collected; thus, less deflection of the air stream occurred, and the collection efficiencies of this investigation were probably higher than those indicated in the table.

The spillover sampling method was calibrated with Diesel fuel and found to be accurate to within ±5 percent (ref. 3). The method was also calibrated as a part of this investigation. The injection of water into

saturated air streams ensured no evaporation of the injected liquid. The water-injection rate, as determined from spillover sampling measurements across the duct, was compared with the metered water input to establish the sampling efficiency.

Over wide ranges of air-flow and water-flow conditions, sampling was found to account for about 90 percent of the metered input. This value includes the effects of droplet collection efficiency as well as other errors inherent in the determination of an average concentration across a duct. This sampling efficiency of 90 percent was used to correct the spillover sampling measurements of this investigation.

The concentration of the fuel vapor captured along with the fuel droplets in the spillover sample was included in the liquid fuel-air ratio indicated by the conductivity-type mixture analyzer. In this program, all the liquid fuel-air ratio measurements were corrected to account for entrained vapor fuel. The analysis by which this correction was obtained is described in the appendix.

Experimental Procedure

Each run consisted of a nonspillover and a spillover sampling traverse. All traverses included nine sampling points spaced across the diameter of the duct. Sampling at stream velocity was accomplished by regulating the sample gas-flow rate until the flow rate indicated by the rotameter equalled the calculated flow rate intercepted by the probe. The spillover samples were then taken with a sample gas flow of about 40 percent of the nonspillover rate. However, this flow rate could be varied over a range of 20 to 60 percent of the nonspillover rate without appreciably affecting the calculated liquid fuel-air ratios. To reduce the fuel-air ratio of the spillover samples to a value within the range of the analyzer, measured quantitites of diluent air were added.

The zero setting of the NACA mixture analyzer was checked before and after each traverse. The analyzer calibration was also checked periodically with a standard gas sample. During all traverses a gage pressure of about 2 inches of mercury was maintained at the analyzer inlet. For runs in which the air preheater was used, the fuel-air ratio that resulted from the combustion products of the JP-4 fuel was determined before the isooctane flow was started. This small fuel-air ratio value was deducted from each of the measured total fuel-air ratios.

Calculations

Each fuel-air-ratio measurement of each traverse was plotted against the square of the distance from the spray axis at which the measurement

was made. From these plots, the average fuel-air ratio of each profile was determined by graphical integration. In this calculation, the spray was assumed symmetric about the spray axis, and the air-velocity profile in the region of the spray was assumed flat. The latter assumption was known from measurements of the velocity profile to be sufficiently valid over the region in which samples were taken.

The average fuel-air ratios were compared with the over-all fuel-air ratio computed from the metered air- and fuel-flow rates. The degree of spray evaporation was thus determined by a comparison of the average liquid fuel-air ratio with the metered fuel-air ratio. The precision of the run was indicated by the agreement of the two total fuel-air ratios.

A semilog plot of fuel-air ratio against the square of the distance from the spray axis was drawn for each total fuel-air-ratio profile. The fuel-spray spreading index of the profile was obtained from the slope of a straight line faired through the data points.

RESULTS AND DISCUSSION

Data on the percentage of evaporation and the degree of spreading of isooctane fuel sprays were obtained by sampling the fuel-air mixture across an 8-inch-diameter duct. Each run consisted of measurements of both the total and the liquid fuel-air ratio distribution. A typical set of fuel-distribution profiles is presented in figure 3. A summary of the experimental data is presented in table I.

From the measurements shown in figure 3, an average total fuel-air ratio equal to 0.00445 was calculated. This total fuel-air ratio deviated from the metered over-all fuel-air ratio by 8.8 percent. In most instances, the average total fuel-air ratio obtained from the distribution profiles agreed within ±10 percent with the metered over-all fuel-air ratio. Both the total and the liquid fuel-air-ratio profiles were reproducible to within ±5 percent.

Degree of Spray Evaporation

The degree of spray evaporation, expressed in percentage of fuel evaporated, was determined from a comparison of the average liquid fuel-air ratio with the metered over-all fuel-air ratio. In figure 3, 54.6 percent of the injected fuel was found to be evaporated.

The influence of each experimental variable on spray evaporation was studied while the other five experimental variables were maintained fixed. With the fuel-injection system used in this study, the degree of atomization of the injected fuel was determined by both the inlet-air

and the fuel-injection parameters. Since spray evaporation was dependent on the degree of atomization, the influence of each experimental variable on the evaporation rate included both its effect on the atomization process and any additional effect on the evaporation process.

Effect of air temperature. - The influence of air temperature on the degree of spray evaporation is shown in figure 4. These measurements were obtained with several fixed air velocities and at a distance of $10\frac{3}{8}$ inches from the 0.041-inch-diameter fuel orifice. The air pressure and the fuel pressure drop were maintained at 25 inches of mercury absolute and 55 pounds per square inch, respectively.

The large increase in evaporation rate with air temperature may be attributed to the greater heat transfer to the evaporating liquid as the temperature difference between the air and droplets was increased. Also, as the air density was diminished, greater upstream penetration of the spray and, thus, longer residence times were possible.

Effect of air velocity. - The degree of spray evaporation was also found to increase with air velocity as shown in figure 5. However, the influence of air velocity was considerably smaller than that of air temperature. The data were obtained at four fixed air temperatures and under the same conditions as those of figure 4.

The influence of air velocity was probably the result of a combination of factors. Finer atomization of the injected fuel and higher heat-transfer coefficients between the air and droplets would be expected at the higher air velocities. Increased spray evaporation would result from both of these factors. However, greater air velocities would also be expected to decrease the residence time of the sprays. The results of figure 5 indicate that the gains in the degree of evaporation resulting from greater air velocities overbalanced the effects of shorter residence times.

Effect of air pressure. - The degree of spray evaporation decreased as the air pressure was increased (fig. 6). In this series, the 0.041-inch-diameter orifice and a fuel-pressure drop of 55 pounds per square inch were employed. The samples were withdrawn at a distance of $10\frac{3}{8}$ inches from the orifice at four combinations of constant air temperature and velocity.

The decrease in evaporation with increase in air pressure is partially explained by the fact that the surface temperature of the drops is increased as the ambient-air pressure is increased, and as a result the heat transfer to the drops is decreased. This fact is proved experimentally for single droplets in reference 6. Also, as the air density increased, the spray residence time was probably diminished as a result of shorter upstream penetration.

Effect of axial distance from fuel injector. - The results of sampling at three axial distances from the fuel injector are shown in figure 7. These determinations were made with several combinations of constant air temperature and velocity and at an air pressure of 25 inches of mercury absolute. The fuel-injection pressure drop across the 0.041-inch-diameter orifice was maintained at 55 pounds per square inch. The gains in the degree of evaporation with distance were due solely to the increased spray residence times, since, for a given set of conditions, the fuel atomization was fixed.

Effect of fuel-injection pressure drop. - The effect of fuel-injection pressure drop across the 0.041-inch-diameter orifice is shown in figure 8. The pressure drop was varied from 25 to 85 pounds per square inch; and the data were obtained at an axial distance of $10\frac{3}{8}$ inches from the injector, a static pressure of 25 inches of mercury absolute, and three combinations of constant air temperature and velocity. The higher degree of evaporation obtained as the injection pressure was increased may be attributed to the finer atomization and deeper upstream penetration that probably occurred because of the higher pressure drop.

Effect of diameter of fuel orifice. - The degree of spray evaporation was essentially unaffected by changes in the diameter of the fuel orifice (fig. 9). Evaporation rates were determined at three combinations of air temperature and velocity, an air pressure of 25 inches mercury absolute, a sampling distance of $10\frac{3}{8}$ inches, and a fuel-injection pressure drop of 55 pounds per square inch.

As the nozzle size was decreased, finer atomization and shorter upstream penetration of the spray probably resulted. Apparently, the gains in the degree of spray evaporation due to the finer atomization were essentially counteracted by the influence of the decreased penetration which reduced the residence time.

Correlation of results. - The degree of spray evaporation is related to the experimental variables in figure 10. This relation, which was found to be valid over the investigated ranges of experimental conditions, may be expressed as follows:

$$\frac{N}{100 - N} = 9.35\left(\frac{T_a}{1000}\right)^{4.4}\left(\frac{V_a}{100}\right)^{0.80} p_a^{-1.2}\, p_f^{0.42}\, L^{0.84}$$

The term $\frac{N}{100 - N}$ was used in the correlation, because the degree of spray vaporization N did not exhibit a constant proportionality to the experimental variables. With this term, however, the exponents of the five variables are indicative of the actual dependence of N on the

experimental parameters, since $\frac{N}{100 - N}$ considerably magnifies the effects of changes in the experimental variables. As an example, N is proportional, over part of the investigated range, to about the 1.5 power of the air temperature as compared with the 4.4 power relation of $\frac{N}{100 - N}$.

The equation is significant because it shows the relative importance of each of the inlet-air and fuel-injection parameters. The extremely large influence of air temperature is evident. In comparison, the effects of the other variables, particularly that of fuel-injection pressure drop, are minor.

3068

Fuel-Spray Spreading

The second major consideration of the fuel preparation process is the distribution pattern of the fuel spray. An equation which describes the diffusion of fuel from a continuous point source in high velocity air streams is reported in reference 7. The modified form of this equation, presented in reference 3, may be further simplified to give

$$f_t = \frac{f_o R^2}{M} \exp\left(-\frac{r^2}{M}\right)$$

This equation predicts a straight-line relation between the logarithm of fuel-air ratio and the square of the radial distance from the spray axis. The slope of this line is represented by $-1/M$.

The total fuel-air-ratio distribution of figure 3 is presented in a semilog plot in figure 11. The slope of the straight line was -90.8 per square foot. The positive reciprocal value of the slope M of each total fuel-air-ratio profile was used as an index of fuel-spray spreading. This index is directly proportional to the degree of spreading. An index of this type was considered a more suitable criterion of the influence of each of the experimental variables on fuel spreading than a fictitious diffusion coefficient. In a heterogeneous system, as in the sprays employed in this program, a diffusion coefficient is not generally applicable.

The effect of each of the experimental parameters on the spreading index was determined as a part of the evaporation-rate determinations. The fixed sets of variables with which the influence of each variable was studied were therefore identical to those described for the evaporation measurements. These experimental conditions are given in the figures in which the spreading indices are presented.

Effect of air temperature. - The direct relation between spreading index and air temperature is illustrated in figure 12. This increase in spreading with increasing air temperature may be attributed to changes in the spray penetration. The upstream penetration of the spray probably increased as the air density was decreased. This factor would cause longer residence times and more initial radial dispersion of the fuel droplets.

Effect of air velocity. - The data presented in figure 13 show that the spreading index decreased with increasing air velocity. This decrease in the spreading apparently resulted from the shorter residence times of the spray. The data also indicate that less initial radial penetration of the liquid was obtained as the atomization became finer.

Effect of air pressure. - The influence of the ambient pressure on the index of fuel spreading is shown in figure 14. The results demonstrate that the degree of spreading diminished as ambient pressures were increased. Shorter residence times due to the reduced upstream penetration of the fuel probably resulted as the air density was increased.

Effect of axial distance from fuel injector. - The index of spreading was found to have a direct relation to axial distance from the nozzle (fig. 15). Since all other conditions were fixed, this effect of distance was solely a result of longer residence times.

Effect of fuel-injection pressure drop. - The spreading index increased with increasing injection pressures as illustrated in figure 16. At the higher pressure drops, deeper upstream spray penetration probably occurred and resulted in a greater degree of fuel spreading. However, finer atomization, and thus lessened radial penetration, would also be expected as the injection pressures were increased. Apparently, the influence of the increased penetration overbalanced the effect of finer atomization.

Effect of diameter of fuel orifice. - Although no effect was observed on evaporation, the spreading index exhibited a direct dependence on the diameter of the fuel orifice (fig. 17). As the orifice size was enlarged, coarser atomization and deeper penetration probably resulted; both of these factors would tend to increase fuel spreading. In the case of spray evaporation, however, these two factors would tend to cancel out.

Correlation of results. - In figure 18, the index of fuel-spray spreading is related to the six experimental parameters. This relation was found to be suitable over the ranges of experimental conditions studied. The straight line of figure 18 may be represented by the following equations:

$$M = 0.0598\Phi + 0.00042$$

and

$$\Phi = \frac{\left(\frac{T_a}{1000}\right)^{0.67} L^{0.76} p_f^{0.49} D^{0.79}}{\left(\frac{V_a}{100}\right)^{0.85} p_a^{0.57}}$$

This expression indicates which factors are significant in determining the fuel spreading. Spray residence time apparently is of major importance, since the effect of L was solely, and the effect of V_a mainly due to this factor. If the exponents of L and V_a were assumed equal, these two parameters could essentially be replaced by a residence time to about the 0.80 power. The influence of the other four variables was also due in part to changes in the residence time of the sprays through changes in upstream penetration distance.

RESULTS AND CONCLUSIONS

The results of this investigation are limited to the case of upstream injection of isooctane from a simple orifice. However, the relations can probably be extended to any gasoline-type fuel without serious error. The fuel-spreading results are further limited to the levels of turbulence that prevailed in the test duct. For application to engine design, these results therefore represent the minimum degree of spreading, since higher turbulence levels would normally be encountered in engines.

The major contribution of this study was the determination of the relative effect of each of the inlet-air and fuel-injection parameters on the evaporation and the mixing of volatile fuels in high-velocity air streams. The results indicate that evaporation of these fuels occurs readily, even in short axial distances from the fuel nozzle. Therefore, evaporation does not appear to be a controlling step in the combustion process in ram-jet engines with inlet-temperatures higher than 200° F.

The distribution profiles of isooctane injected contrastream from simple-orifice fuel injectors into high-velocity air streams were determined by sampling measurements across a duct 8 inches in diameter. Over the ranges of inlet-air and fuel-injection parameters investigated, the following relations were obtained:

1. The degree of spray evaporation was related to the experimental variables by the following equation:

$$\frac{N}{100 - N} = 9.35 \left(\frac{T_a}{1000}\right)^{4.4} \left(\frac{V_a}{100}\right)^{0.80} p_a^{-1.2} p_f^{0.42} L^{0.84}$$

where N is the percent of spray evaporation, T_a is the inlet-air temperature in $^{\circ}R$, V_a is the inlet-air velocity in feet per second, p_a is the inlet-air pressure in inches of mercury absolute, p_f is the fuel-injection pressure drop in pounds per square inch, and L is the axial distance from the fuel injector in inches.

2. An index of the degree of fuel-spray spreading was expressed in terms of the experimental variables by the following equations:

$$M = 0.0598\Phi + 0.00042$$

$$\Phi = \frac{\left(\frac{T_a}{1000}\right)^{0.67} L^{0.76} p_f^{0.49} D^{0.79}}{\left(\frac{V_a}{100}\right)^{0.85} p_a^{0.57}}$$

where M is the index of fuel-spray spreading in square feet and D is the diameter of the fuel-injector orifice in inches.

Lewis Flight Propulsion Laboratory
National Advisory Committee for Aeronautics
Cleveland, Ohio, September 17, 1953

APPENDIX - CALCULATION OF LIQUID FUEL-AIR RATIO

The liquid fuel-air ratio measurements indicated by the conductivity-type mixture analyzer included the concentration of vapor fuel which was captured along with the liquid fuel droplets. The following analysis was employed to obtain the true liquid fuel-air ratio at the sampling point from the experimental measurements. The following symbols were utilized in this analysis:

c_s concentration of fuel in collected sample after addition of diluent air, lb fuel/lb mixture

f_l liquid fuel-air ratio in main stream at point of sampling

f_s fuel-air ratio of collected sample after addition of diluent air

f_t total fuel-air ratio in main stream at point of sampling

f_v vapor fuel-air ratio in main stream at point of sampling

W_a weight flow of air intercepted by probe, lb/hr

W_a' weight flow of air captured by probe, lb/hr

W_d weight flow of diluent air added to collected sample, lb/hr

W_f weight flow of fuel captured by probe, lb/hr

W_l weight flow of liquid fuel captured by probe, lb/hr

W_s total weight flow of collected sample after addition of diluent air, lb/hr

The sampling efficiency of the spillover method employed in this investigation was found, in a separate study, to be approximately 90 percent. This efficiency was assumed in the analysis.

The weight flow of liquid fuel collected by the probe was equal to the total amount of fuel collected minus any fuel vapor contained in the collected sample. Thus

$$W_l = W_f - W_a' f_v \tag{1}$$

Then

$$W_l = W_s c_s - (W_s - W_d - W_s c_s) f_v \tag{2}$$

or

$$W_l = W_s \frac{f_s}{1+f_s} - \left(W_s - W_d - W_s \frac{f_s}{1+f_s}\right)(f_t - f_l) \tag{3}$$

By definition of sampling efficiency

$$\frac{W_l}{W_a f_l} = 0.90 \tag{4}$$

Substituting equation (4) in equation (3) yields

$$0.9\, W_a f_l = W_s \frac{f_s}{1+f_s} - \left(W_s - W_d - W_s \frac{f_s}{1+f_s}\right)(f_t - f_l) \tag{5}$$

By simplifying, the resulting correction term is obtained

$$f_l = \frac{W_d f_t\,(1+f_s) - W_s\,(f_t - f_s)}{(0.9\,W_a + W_d)(1+f_s) - W_s} \tag{6}$$

All of the quantities of equation (6) were measured except W_a. This quantity was calculated from the known cross-sectional area of the probe opening and the known weight flow of air per unit area in the test duct.

REFERENCES

1. Probert, R. P.: The Influence of Spray Particle Size and Distribution in the Combustion of Oil Droplets. Phil. Mag., ser. 7, vol. 37, no. 265, Feb. 1946, pp. 94-105.

2. Fledderman, R. G., and Hanson, A. R.: The Effects of Turbulence and Wind Speed on the Rate of Evaporation of a Fuel Spray. Rep. No. CM667, Eng. Res. Inst., Univ. Michigan, June 20, 1951. (Contract NOrd 7924, Task UMH-3D, Proj. M604-3, U.S. Navy Dept., Bur. Ord.)

3. Longwell, John P., and Weiss, Malcolm A.: Mixing and Distribution of Liquids in High-Velocity Air Streams. Ind. and Eng. Chem., vol. 45, no. 3, Mar. 1953, pp. 667-677.

4. Gerrish, Harold C., Meem, J. Lawrence, Jr., Scadron, Marvin D., and Colnar, Anthony: The NACA Mixture Analyzer and Its Application to Mixture-Distribution Measurement in Flight. NACA TN 1238, 1947.

5. Langmuir, Irving, and Blodgett, Katherine B.: A Mathematical Investigation of Water Droplet Trajectories. Tech. Rep. No. 5418, Air Materiel Command, AAF, Feb. 19, 1946. (Contract No. W-33-038-ac-9151 with General Electric Co.)

6. Ingebo, Robert D.: Study of Pressure Effects on Vaporization Rate of Drops in Gas Streams. NACA TN 2850, 1953.

7. Towle, W. L., and Sherwood, T. K.: Eddy Diffusion - Mass Transfer in the Central Portion of a Turbulent Air Stream. Ind. and Eng. Chem., vol. 31, no. 4, Apr. 1939, pp. 457-462.

TABLE I. - COMPILATION OF EXPERIMENTAL DATA

[Test-duct cross-sectional area, 0.382 sq ft; fuel temperature at nozzle, 80±5° F]

Run	Air flow, W_a, lb/sec	Air velocity, V_a, ft/sec	Air temperature, T_a, °R	Duct static pressure, p_a, in. Hg abs	Overall fuel-air ratio, f_o	Fuel nozzle pressure drop, p_f, lb/sq in.	Injector orifice diameter, D, in.	Axial distance from injector, L, in.	Sampling deviation,[a] percent	Spray evaporation, N, percent	Index of fuel-spray spreading, M, sq ft
1	2.30	99	546	25.0	0.01206	55	0.041	10.4	-8.7	42.0	0.01206
2	3.38	144	549	25.3	.00823	55	.041	10.4	11.0	45.6	.0188
3	3.44	147	545	25.1	.00808	55	.041	10.4	-0.9	45.8	.0178
4	3.50	150	545	25.0	.00794	55	.041	10.4	-4.8	49.6	.0165
5	4.62	197	545	25.2	.00601	55	.041	10.4	-3.8	49.6	.0130
6	4.68	200	542	25.0	.00594	55	.041	10.4	4.2	58.8	.0132
7	5.69	240	534	24.9	.00488	55	.041	10.4	-8.8	54.6	.0110
8	5.77	246	541	24.9	.00482	55	.041	10.4	0.8	58.9	.0103
9	6.88	292	540	25.0	.00404	55	.041	10.4	-3.0	52.1	.00917
10	3.23	154	613	25.2	.00860	55	.041	10.4	-1.3	55.2	.0175
11	4.06	192	602	25.1	.00684	55	.041	10.4	2.2	58.8	.0178
12	5.01	239	606	25.0	.00555	55	.041	10.4	3.2	64.5	.0130
13	3.42	186	694	25.1	.00813	55	.041	10.4	-3.6	71.2	.0160
14	3.70	201	694	25.1	.00752	55	.041	10.4	-4.4	77.5	.0149
15	4.23	228	689	25.1	.00657	55	.041	10.4	12.0	71.2	.0126
16	4.94	270	693	25.0	.00562	55	.041	10.4	12.8	72.6	.0117
17	2.97	163	788	25.2	.00936	55	.041	10.4	-9.4	86.0	.0170
18	3.15	193	786	25.2	.00882	55	.041	10.4	-2.2	81.4	.0161
19	3.87	239	790	25.2	.00718	55	.041	10.4	2.8	87.4	.0149
20	4.68	287	784	25.2	.00594	55	.041	10.4	.0.7	87.7	.0128
21	4.80	296	777	24.8	.00579	55	.041	10.4	7.4	87.3	.0110
22	5.53	341	784	25.0	.00502	55	.041	10.4	-8.8	89.3	.00980
23	5.60	345	783	25.0	.00496	55	.041	10.4	2.4	89.3	.00990
24	2.99	196	841	25.2	.00930	55	.041	10.4	-9.0	83.0	.0174
25	3.63	244	851	24.9	.00766	55	.041	10.4	-9.8	89.8	.0154
26	4.37	287	841	25.2	.00635	55	.041	10.4	-10.8	96.4	.0129
27	1.86	99	548	20.2	.01492	55	.041	10.4	-4.8	43.6	.0256
28	2.77	161	545	18.4	.01002	55	.041	10.4	-5.3	49.8	.0158
29	4.15	148	545	30.0	.00669	55	.041	10.4	-5.2	40.8	.0146
30	4.85	148	543	35.0	.00573	55	.041	10.4	-2.5	36.7	.0135
31	2.60	200	773	19.7	.01068	55	.041	10.4	-2.3	81.0	.0169
32	3.86	196	778	30.1	.00720	55	.041	10.4	4.0	82.7	.0120
33	4.61	204	778	35.0	.00602	55	.041	10.4	-12.6	71.7	.0127
34	31.3	235	770	20.2	.00888	55	.041	10.4	-0.8	90.8	.0149
35	4.73	240	777	30.1	.00587	55	.041	10.4	2.0	86.6	.0136
36	3.85	294	778	20.0	.00722	55	.041	10.4	0.3	84.0	.0129
37	5.82	296	782	30.2	.00477	55	.041	10.4	-5.0	85.2	.0110
38	3.32	284	882	20.3	.00837	55	.041	10.4	-9.0	90.5	.0145
39	4.16	301	862	23.4	.00668	55	.041	10.4	-11.5	90.0	.0132
40	253	252	864	20.7	.01097	55	.041	10.4	-8.8	92.2	.0152
41	3.45	148	545	25.0	.00806	55	.041	5.25	6.8	32.8	.0127
42	3.40	146	549	25.1	.00818	55	.041	18.25	-6.9	62.5	.0244
43	3.40	145	548	25.2	.00817	55	.041	18.25	5.4		.0239
44	4.58	199	547	24.8	.00607	55	.041	5.25	1.6	38.1	.0103
45	4.55	195	545	25.0	.00611	55	.041	18.25	-1.4	64.2	.0203
46	4.58	197	547	25.0	.00607	55	.041	18.25	5.6		.0215
47	5.73	245	546	25.1	.00485	55	.041	18.25	4.1		.0185
48	4.24	229	686	25.0	.00655	55	.041	18.25	-9.2	74.7	.0203
49	5.00	270	687	25.0	.00555	55	.041	18.25	-4.7	79.1	.0180
50	3.20	194	779	25.3	.00869	55	.041	5.25	-2.2	77.4	
51	4.14	254	781	25.1	.00671	55	.041	5.25	1.9	80.8	.0073
52	3.46	147	542	25.1	.00498	25	.041	10.4	-7.2	37.3	.0105
53	4.66	198	541	25.1	.00369	25	.041	10.4	2.4	39.6	.00877
54	4.65	200	537	25.0	.00725	85	.041	10.4	6.8	48.5	.0152
55	3.22	199	784	25.0	.00535	25	.041	10.4	7.3	71.1	.00995
56	3.23	200	791	25.2	.01041	85	.041	10.4	2.3	81.9	.0172
57	3.65	157	545	24.9	.00228	55	.024	10.4	-8.3	45.3	.00917
58	5.37	145	547	25.0	.00453	55	.033	10.4	-10.8	44.2	.0126
59	4.61	198	545	25.0	.00181	55	.024	10.4	-3.9	45.0	.00848
60	45.1	196	546	24.8	.00339	55	.033	10.4	-0.3		.0110
61	3.24	197	774	25.0	.00471	55	.033	10.4	-8.5	82.1	.0114
62	5.54	346	792	25.0	.00276	55	.033	10.4	-4.7	85.0	.00980

[a]Deviation of sampled total fuel-air ratio from metered fuel-air ratio.

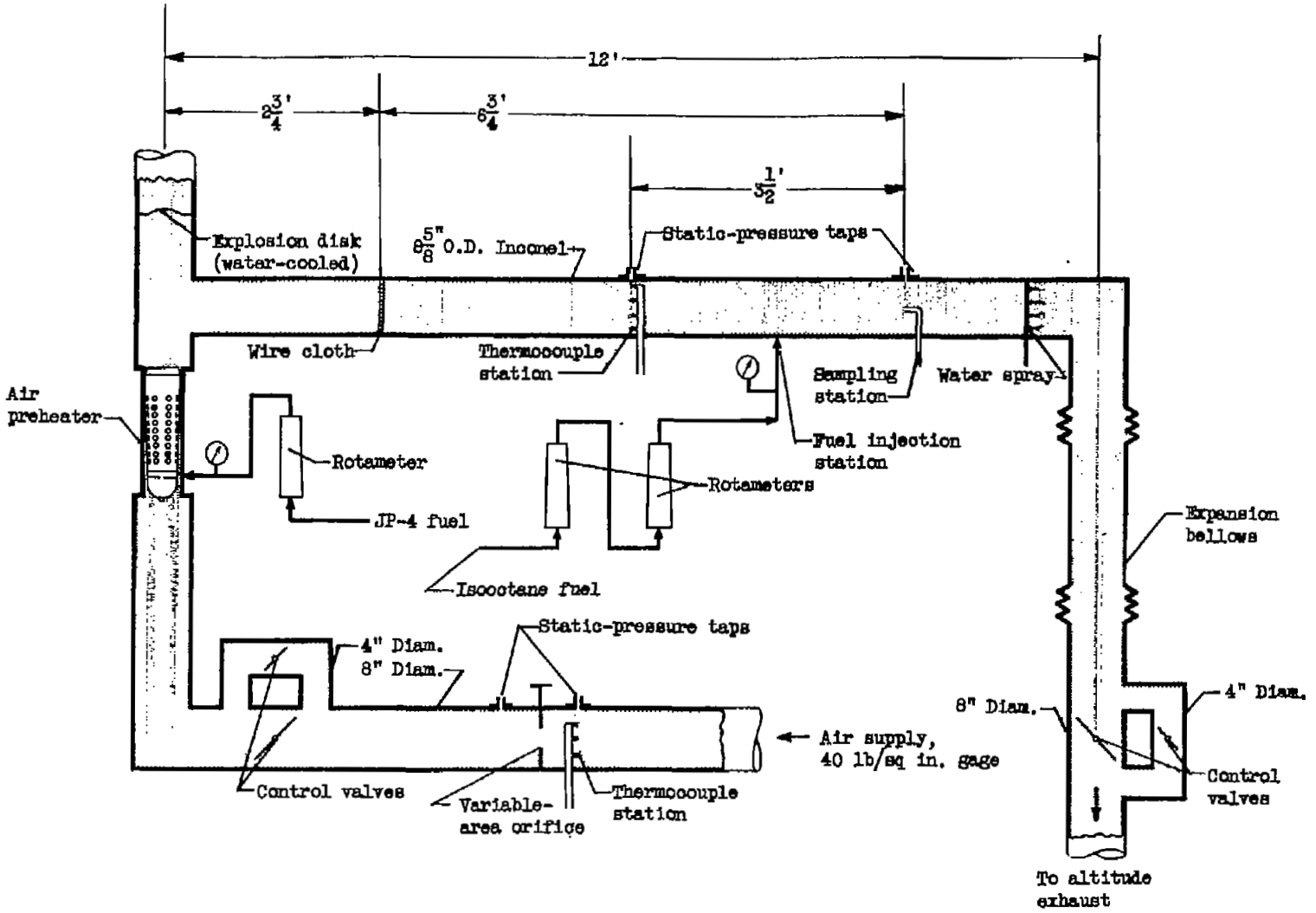

Figure 1. - Schematic drawing of test installation.

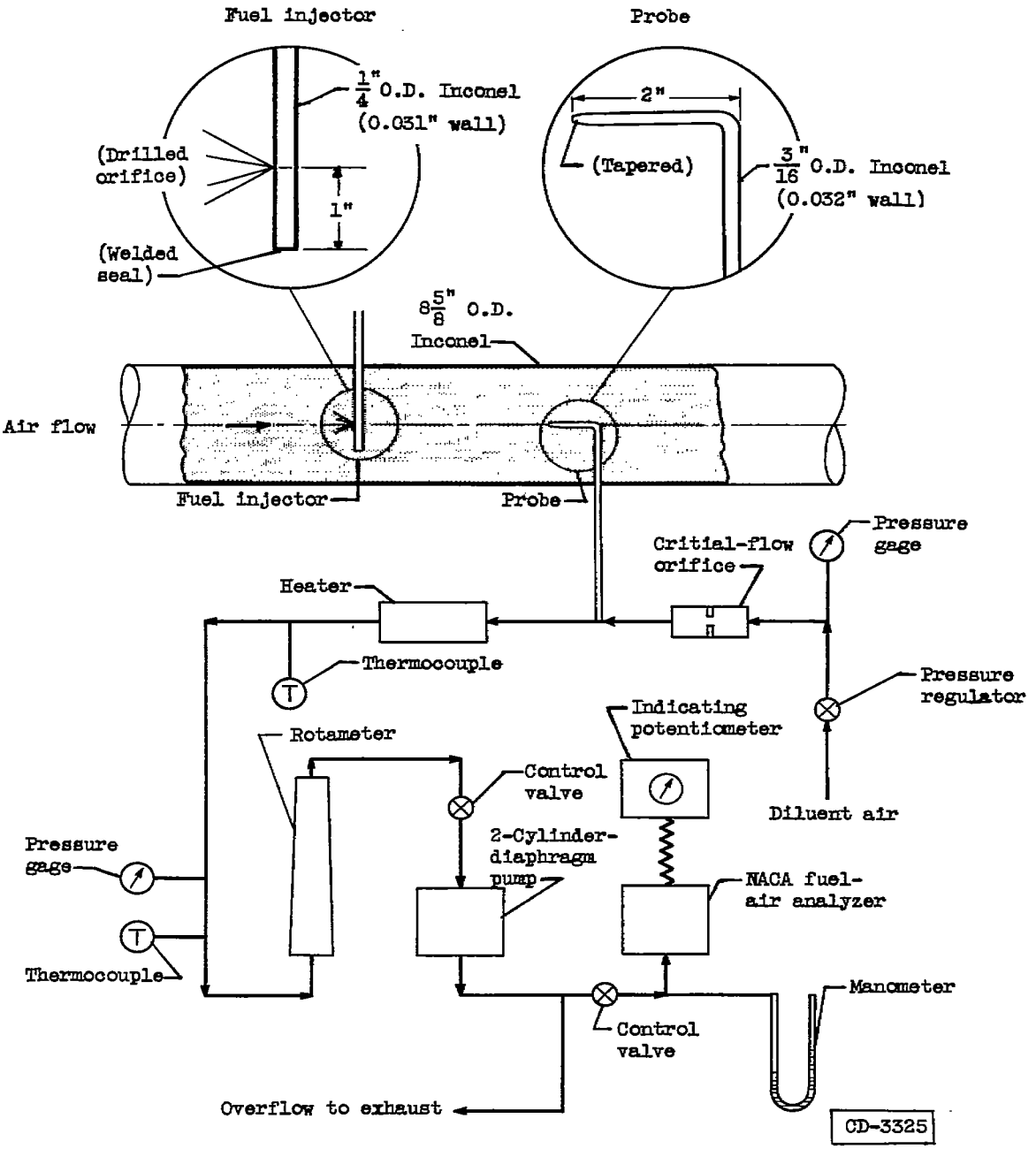

Figure 2. - Schematic diagram of sampling system.

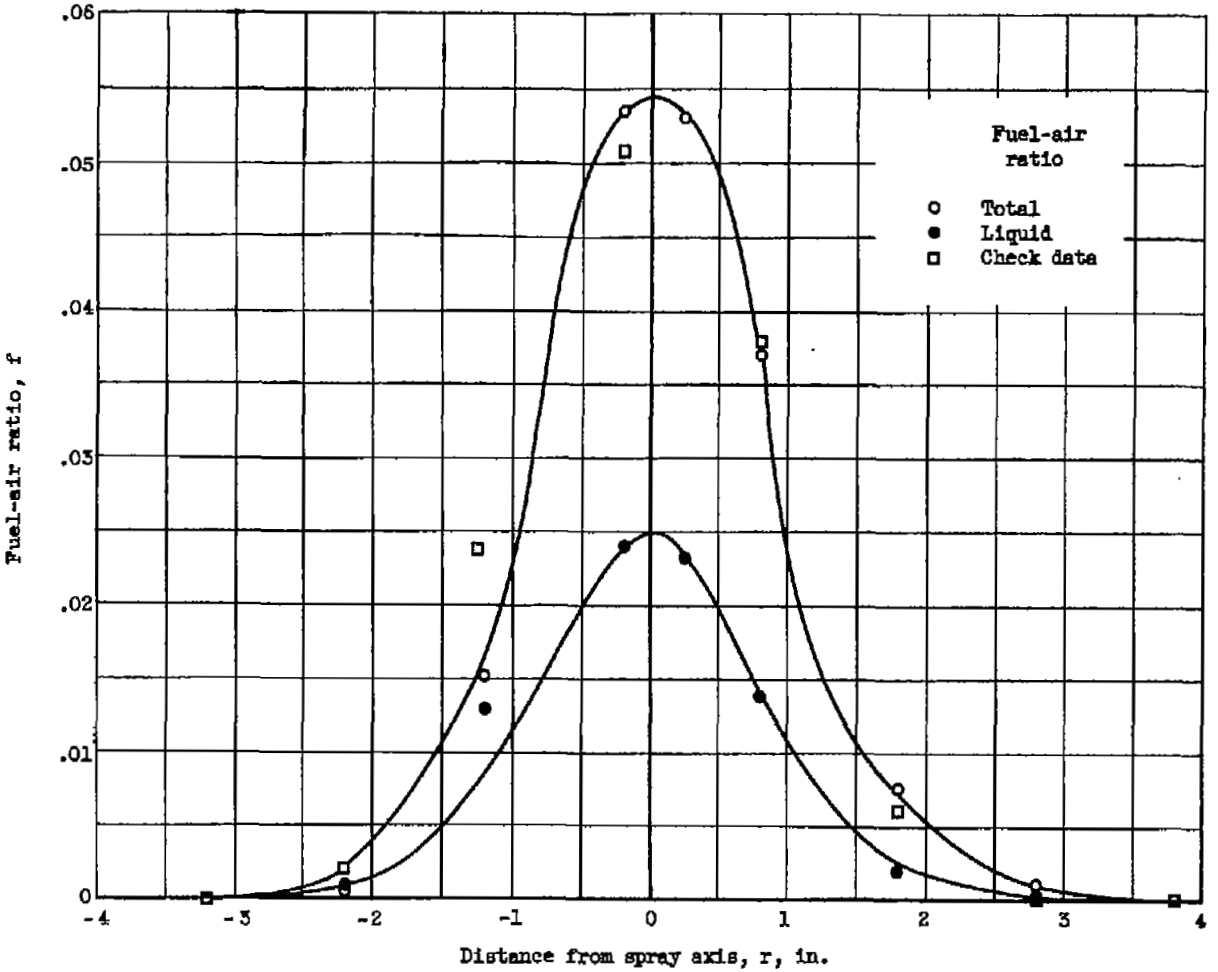

Figure 3. - Typical total and liquid fuel distribution for contrastream injection of isooctane from simple-orifice fuel injector. Fuel evaporated, 54.8 percent; ratio of sampled-to-measured total fuel-air ratio, 0.912; air-flow rate, 5.69 pounds per second; air temperature, 534° R; air velocity, 240 feet per second; air pressure, 24.9 inches of mercury absolute; over-all fuel-air ratio, 0.00488; fuel-injection pressure drop, 55 pounds per square inch; distance from fuel injector, $10\frac{3}{8}$ inches; diameter of fuel-injector orifice, 0.041 inch.

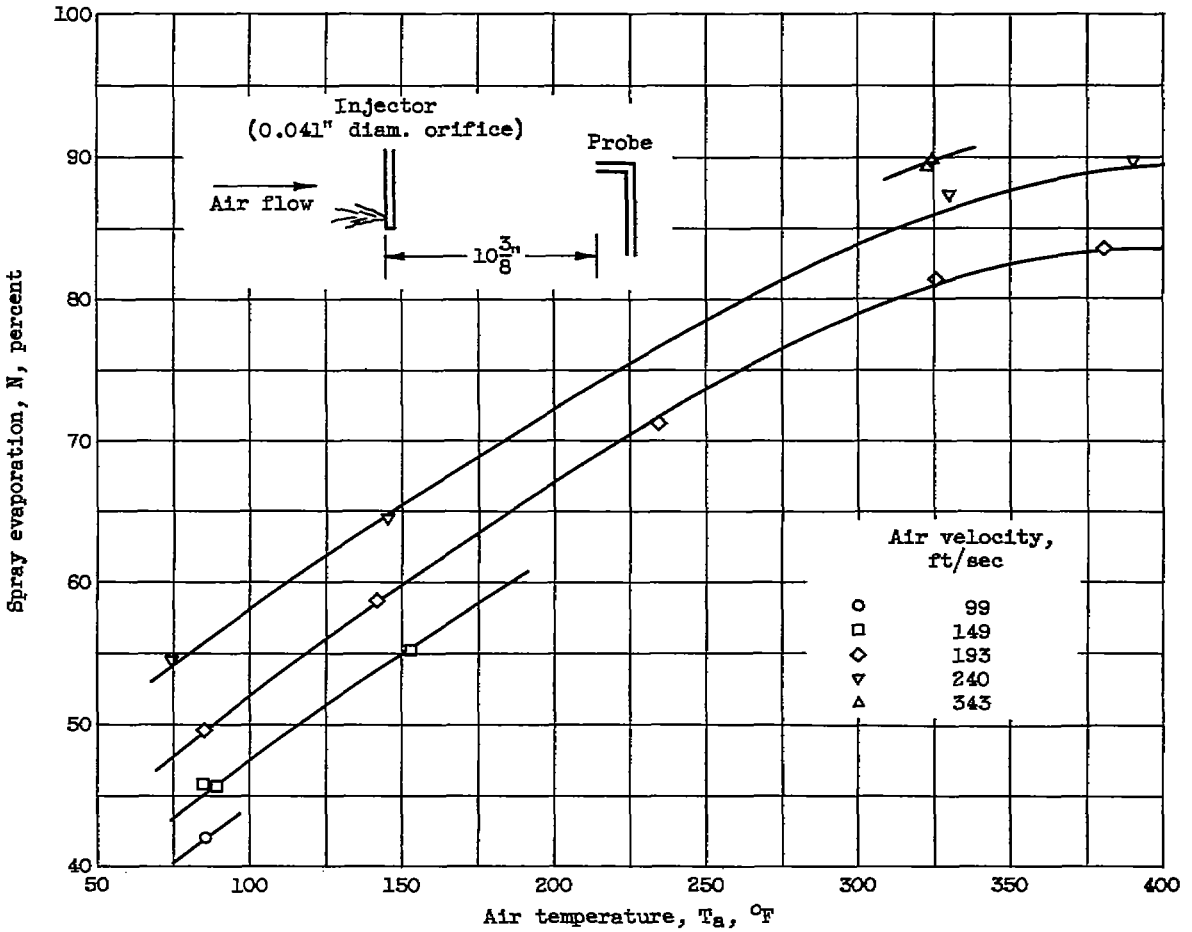

Figure 4. - Effect of air temperature on percentage of fuel spray evaporated. Fuel, isooctane; air pressure, 25 inches of mercury absolute; fuel-injection pressure drop, 55 pounds per square inch.

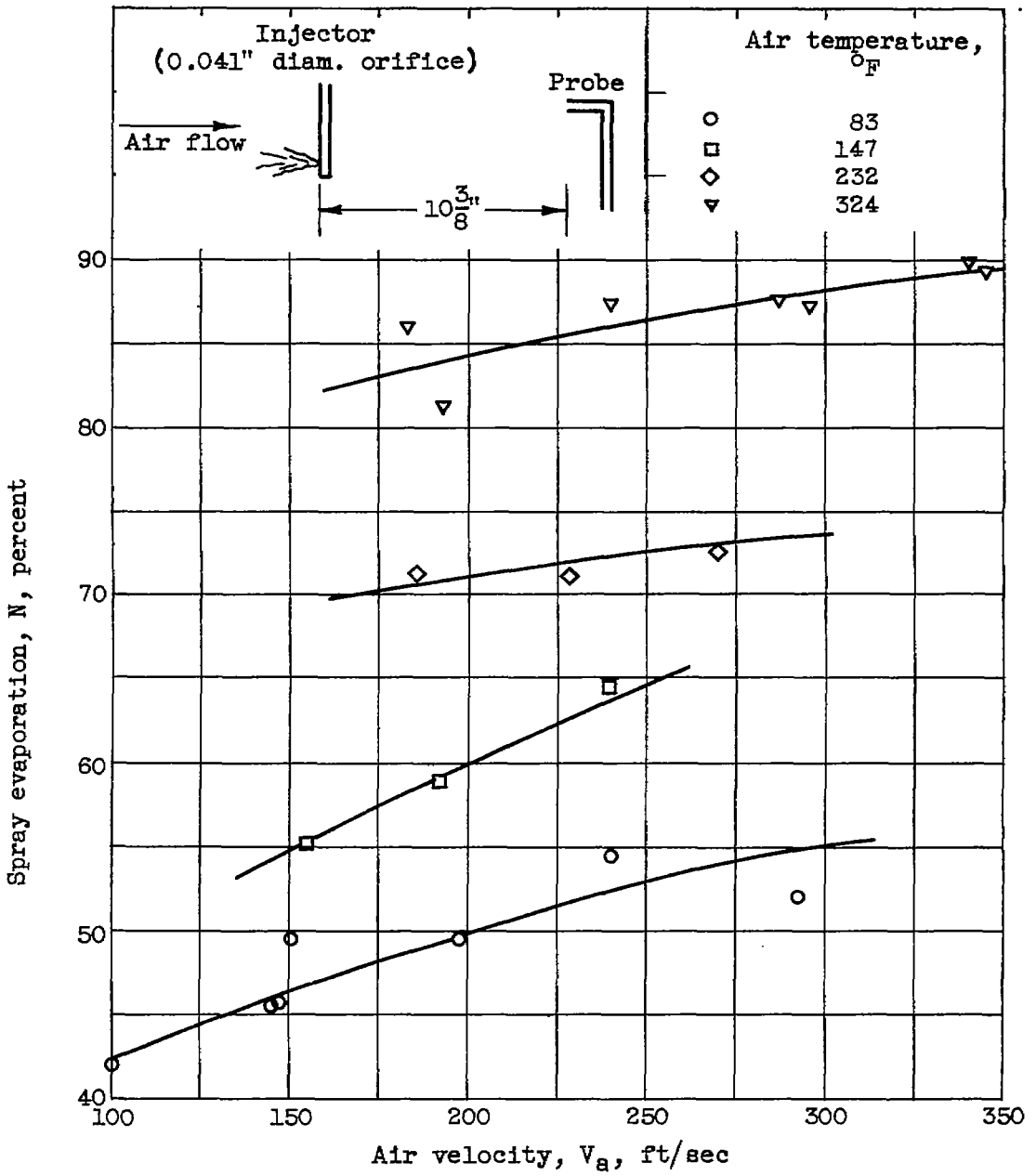

Figure 5. - Effect of air velocity on percentage of fuel spray evaporated. Fuel, isooctane; air pressure, 25 inches of mercury absolute; fuel-injection pressure drop, 55 pounds per square inch.

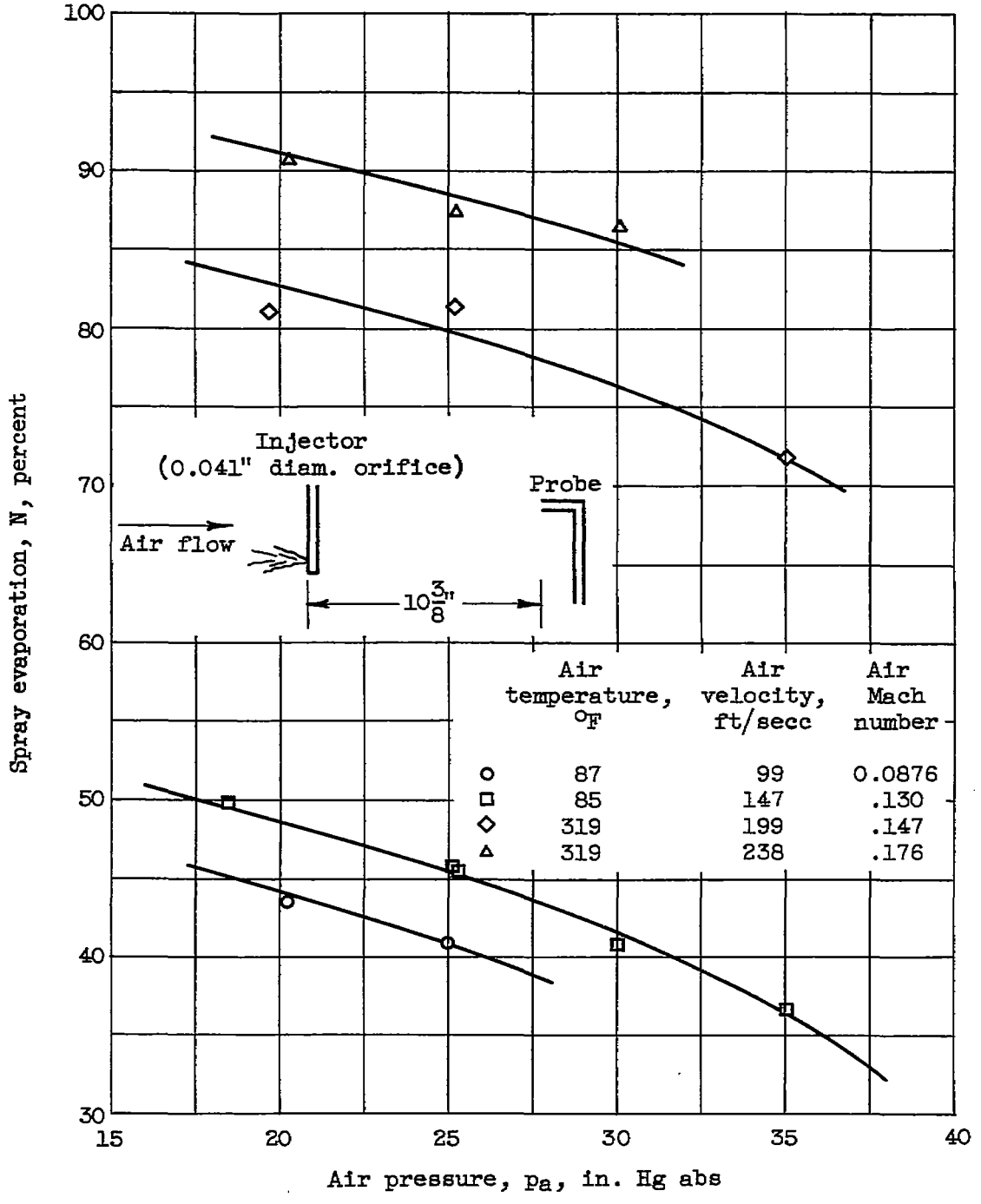

Figure 6. - Effect of ambient pressure on percentage of fuel spray evaporated. Fuel, isooctane; fuel-injection pressure drop, 55 pounds per square inch.

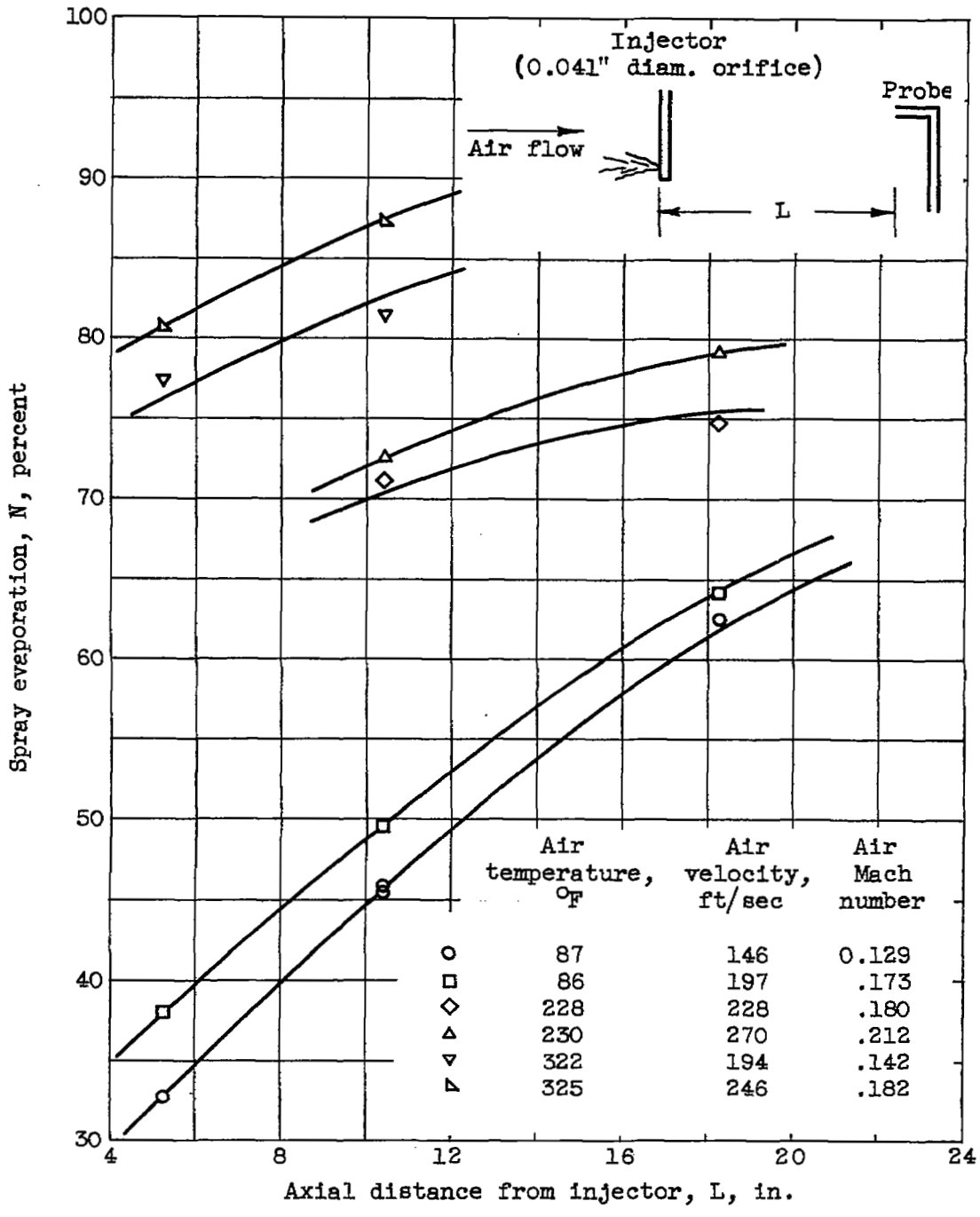

Figure 7. - Effect of sampling distance on percentage of fuel spray evaporated. Fuel, isooctane; air pressure, 25 inches of mercury absolute; fuel-injection pressure drop, 55 pounds per square inch.

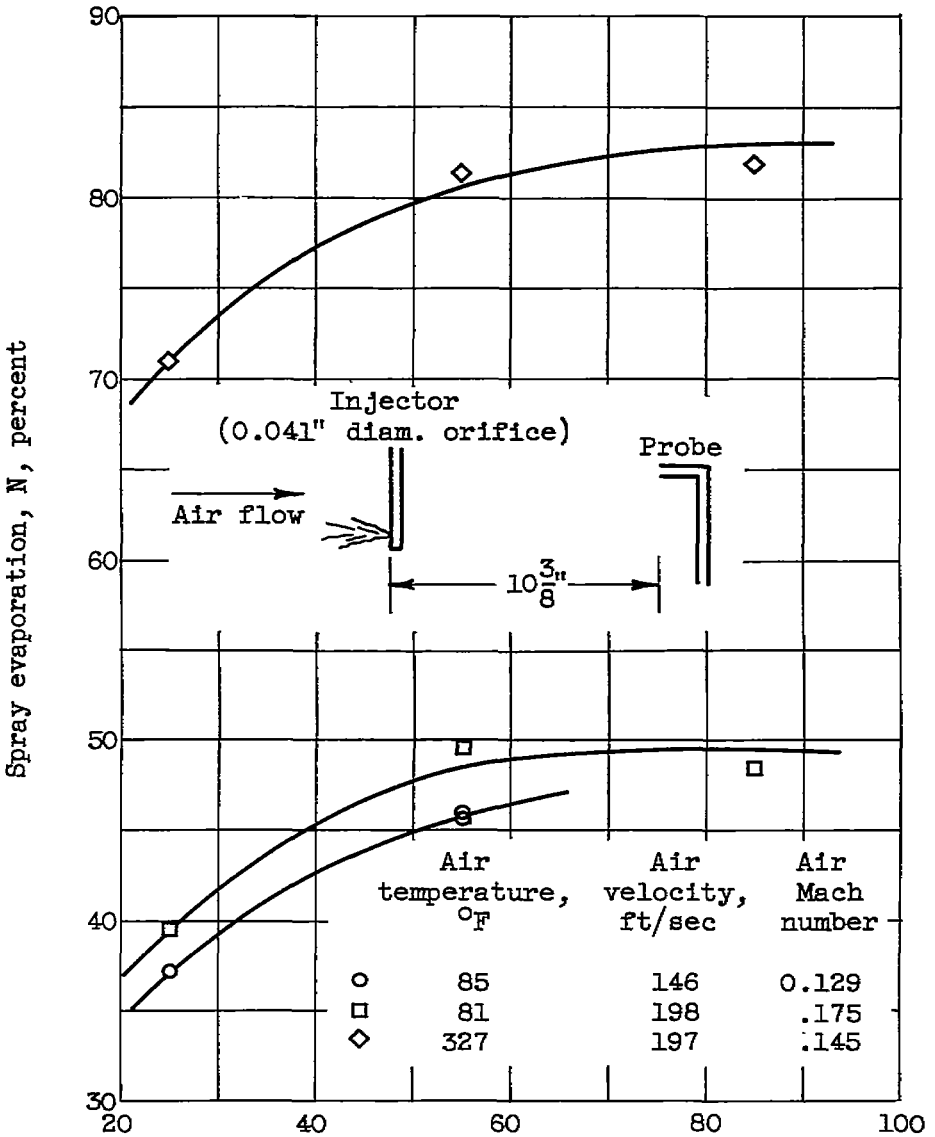

Figure 8. - Effect of fuel-injection pressure drop on percentage of fuel spray evaporated. Fuel, isooctane; air pressure, 25 inches of mercury absolute.

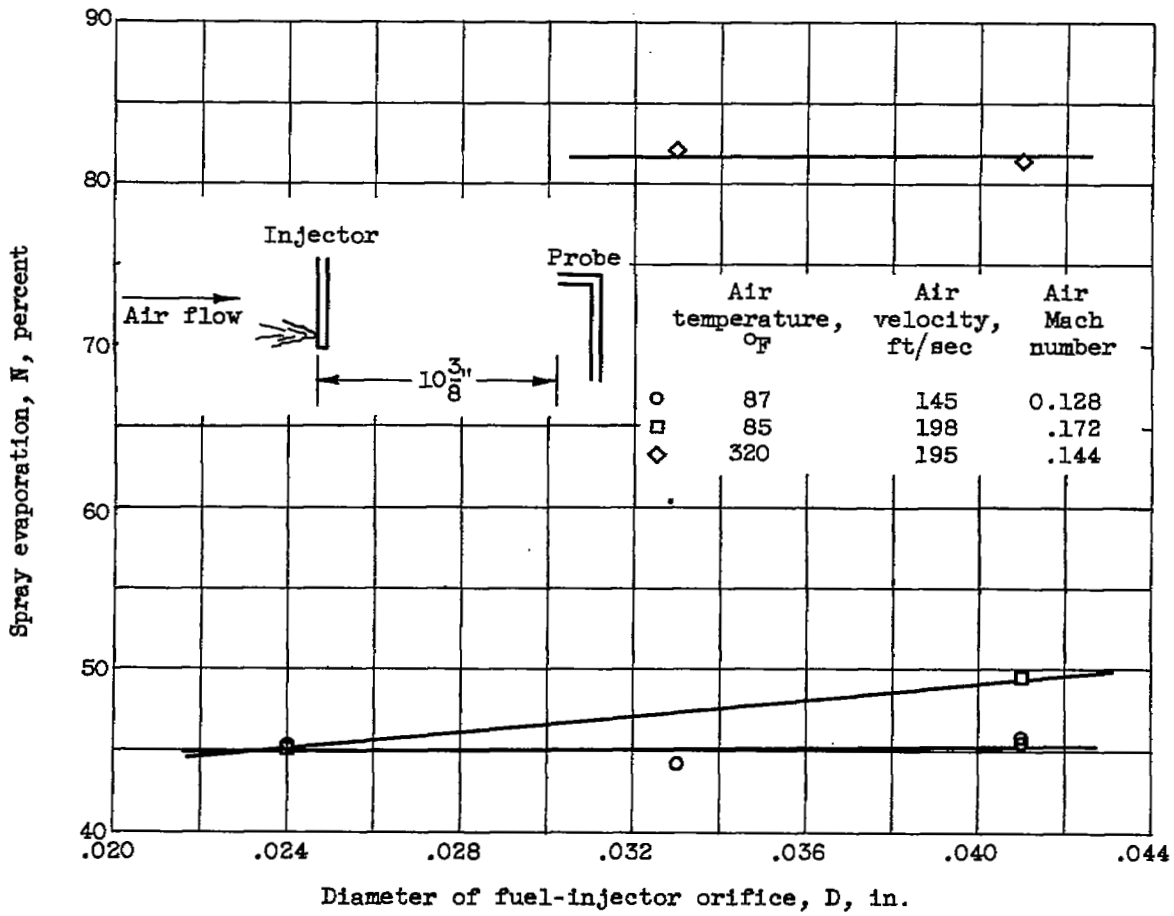

Figure 9. - Effect of orifice size on percentage of fuel spray evaporated. Fuel, isooctane; air pressure, 25 inches of mercury absolute; fuel-injection pressure drop, 55 pounds per square inch.

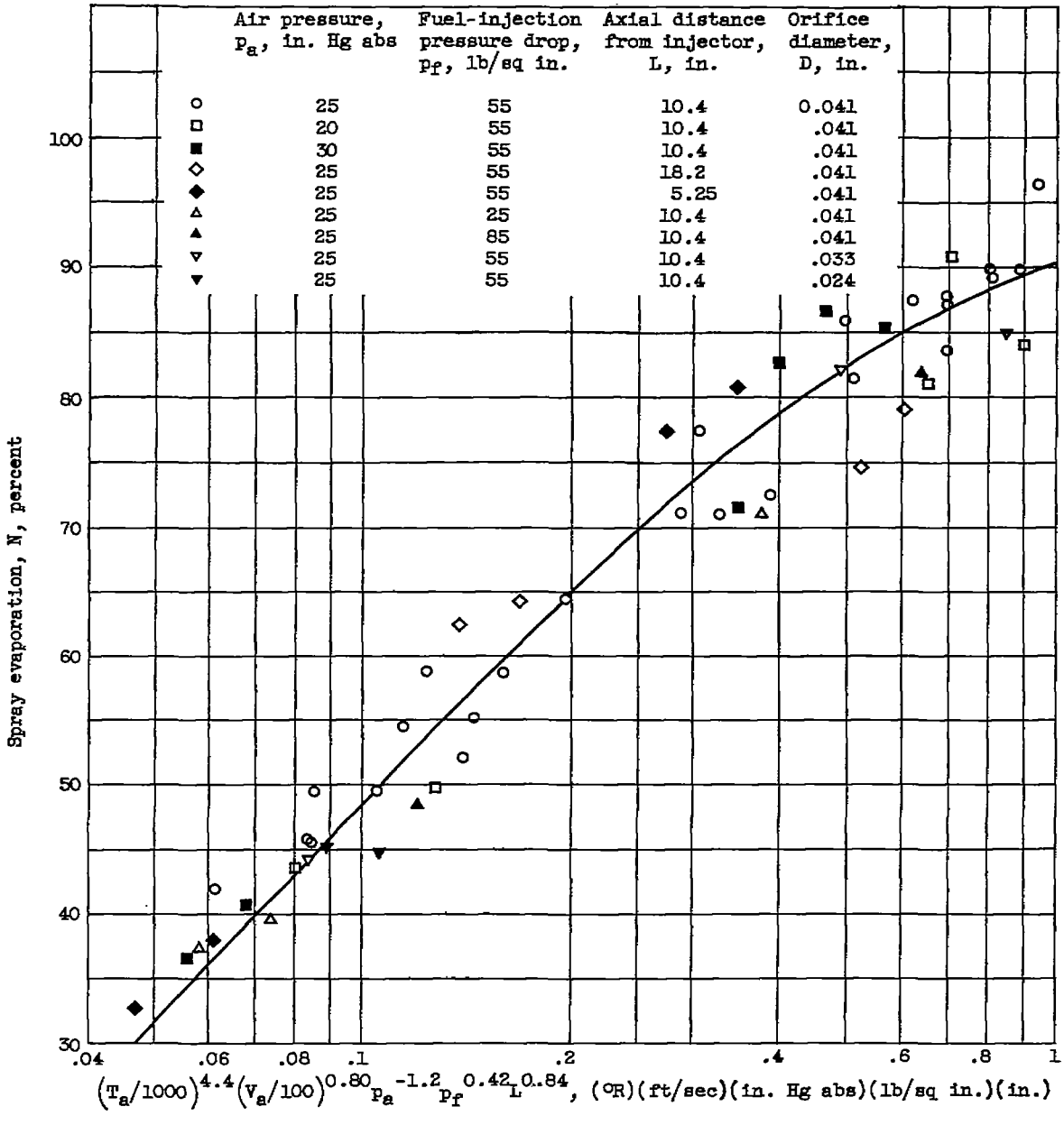

Figure 10. - Correlation of percentage of fuel spray evaporated. Fuel, isooctane; air velocity, 100 to 350 feet per second; air temperature, 80° to 390° F.

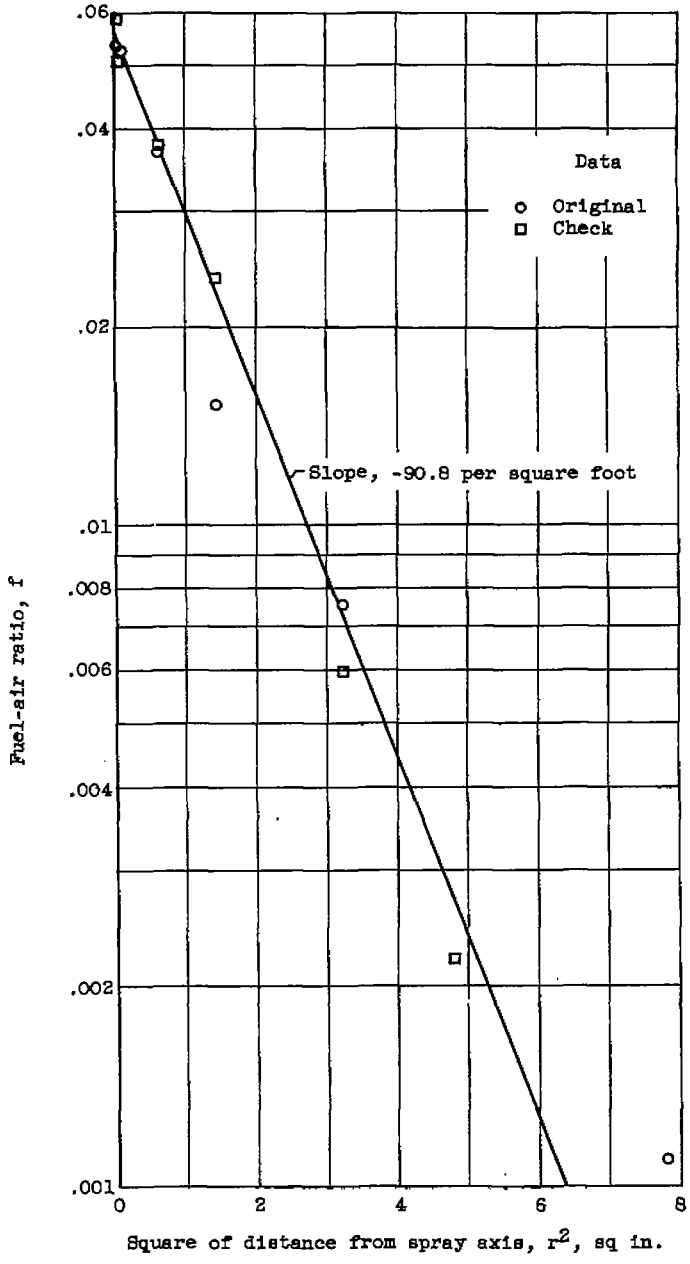

Figure 11. - Typical total fuel distribution for contrastream injection of isooctane from simple-orifice fuel injector. Air flow, 5.69 pounds per second; air temperature, 534° R; air velocity, 240 feet per second; air pressure, 24.9 inches of mercury absolute; over-all fuel-air ratio, 0.00488; fuel-injector pressure drop, 55 pounds per square inch; distance from fuel injector, $10\frac{3}{8}$ inches; diameter of fuel-injector orifice, 0.041 inch; index of fuel-spray spreading, 0.0110 square foot.

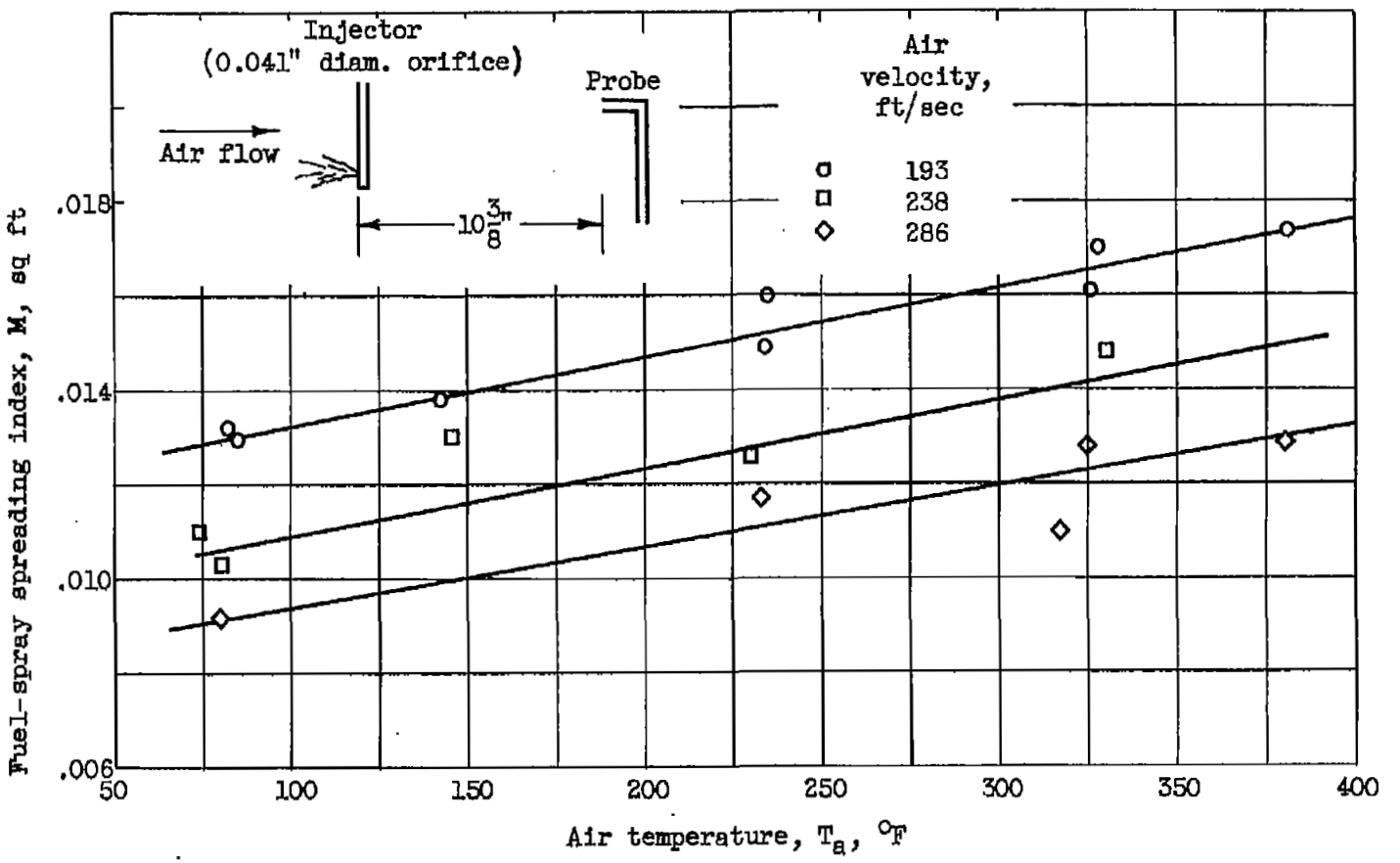

Figure 12. - Effect of air temperature on fuel-spray spreading index. Fuel, isooctane; air pressure, 25 inches of mercury absolute; fuel injection pressure drop, 55 pounds per square inch.

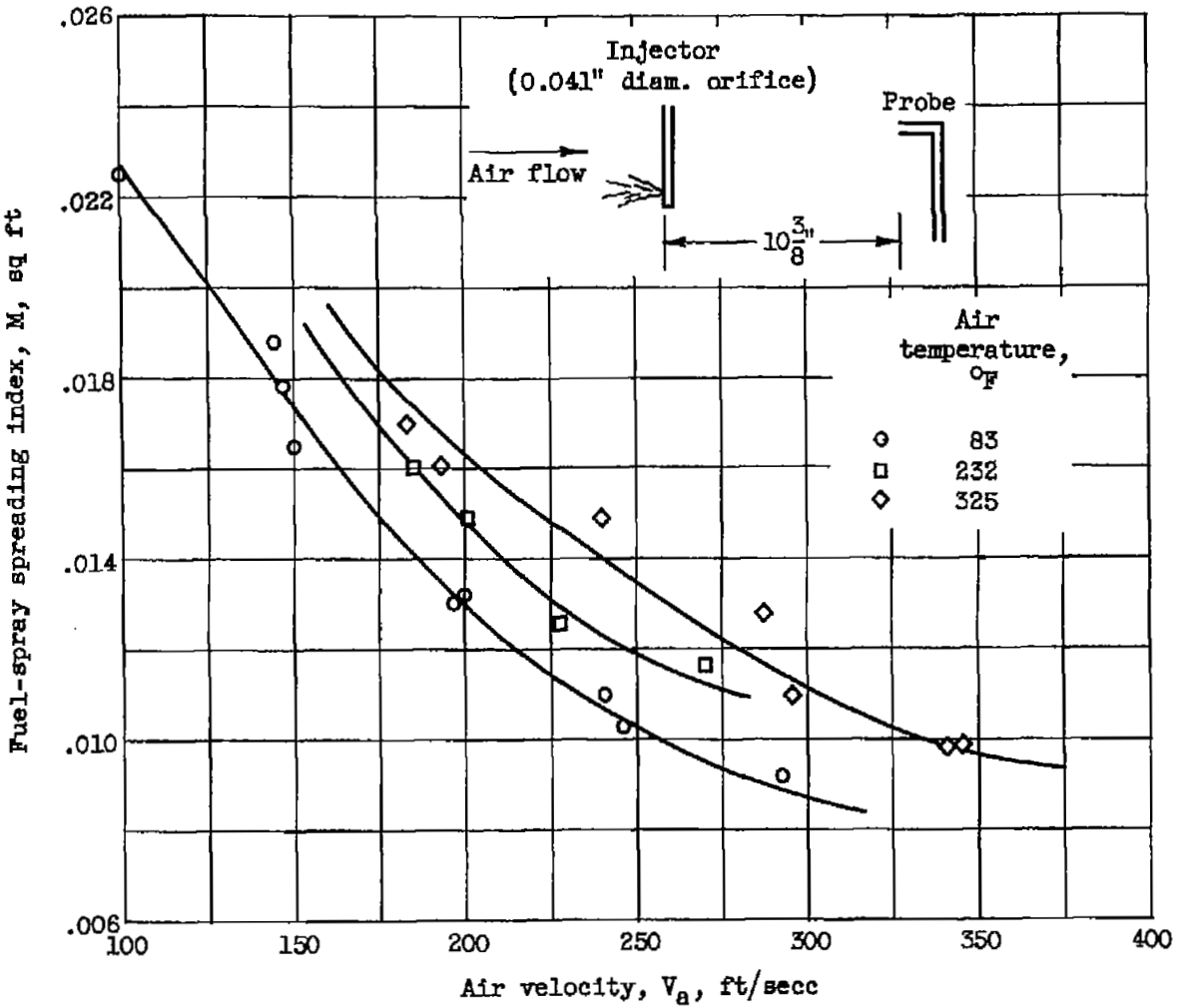

Figure 13. - Effect of air velocity on fuel-spray spreading index. Fuel, isooctane; air pressure, 25 inches of mercury absolute; fuel-injection pressure drop, 55 pounds per square inch.

3068

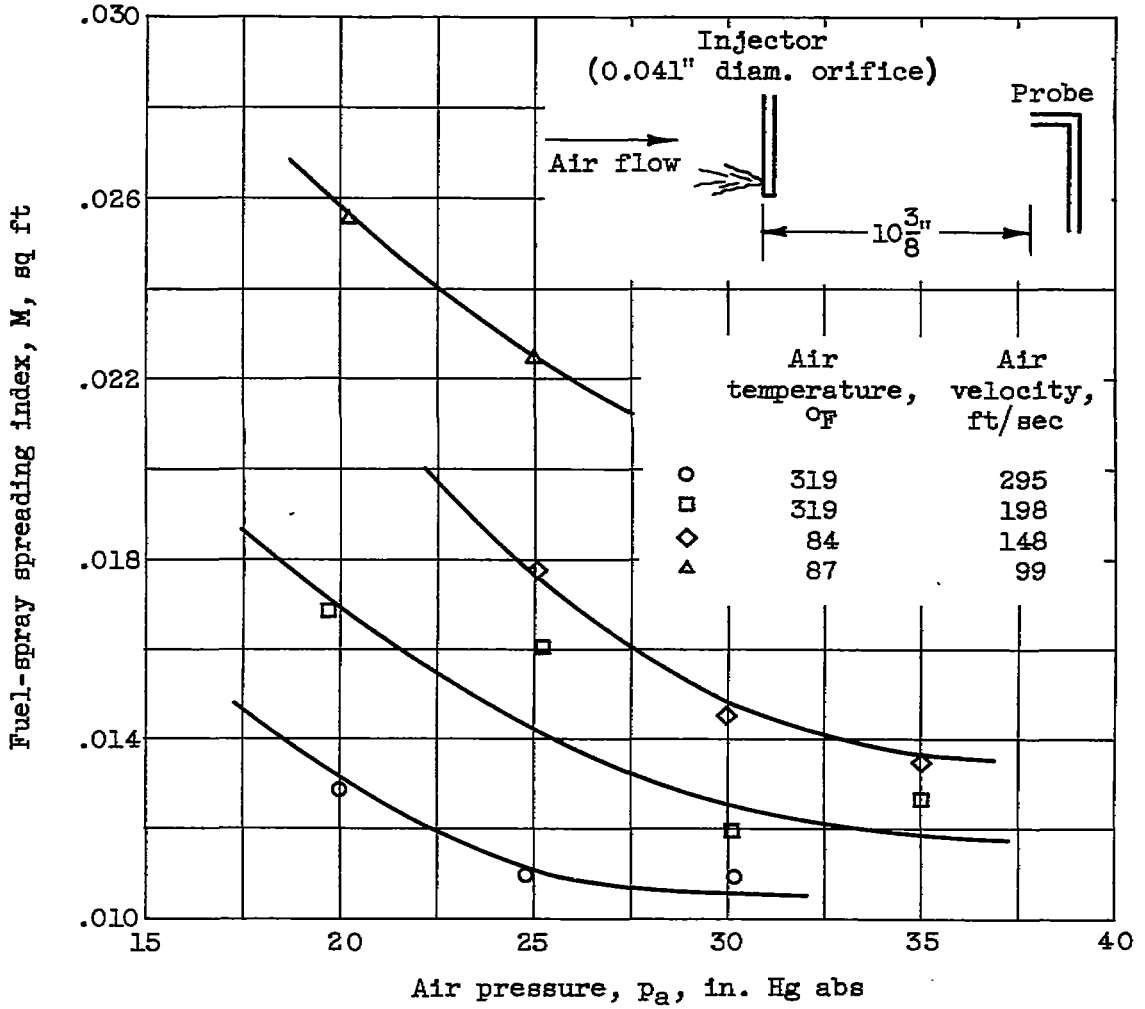

Figure 14. - Effect of air pressure on fuel-spray spreading index. Fuel, isooctane; fuel-injection pressure drop, 55 pounds per square inch.

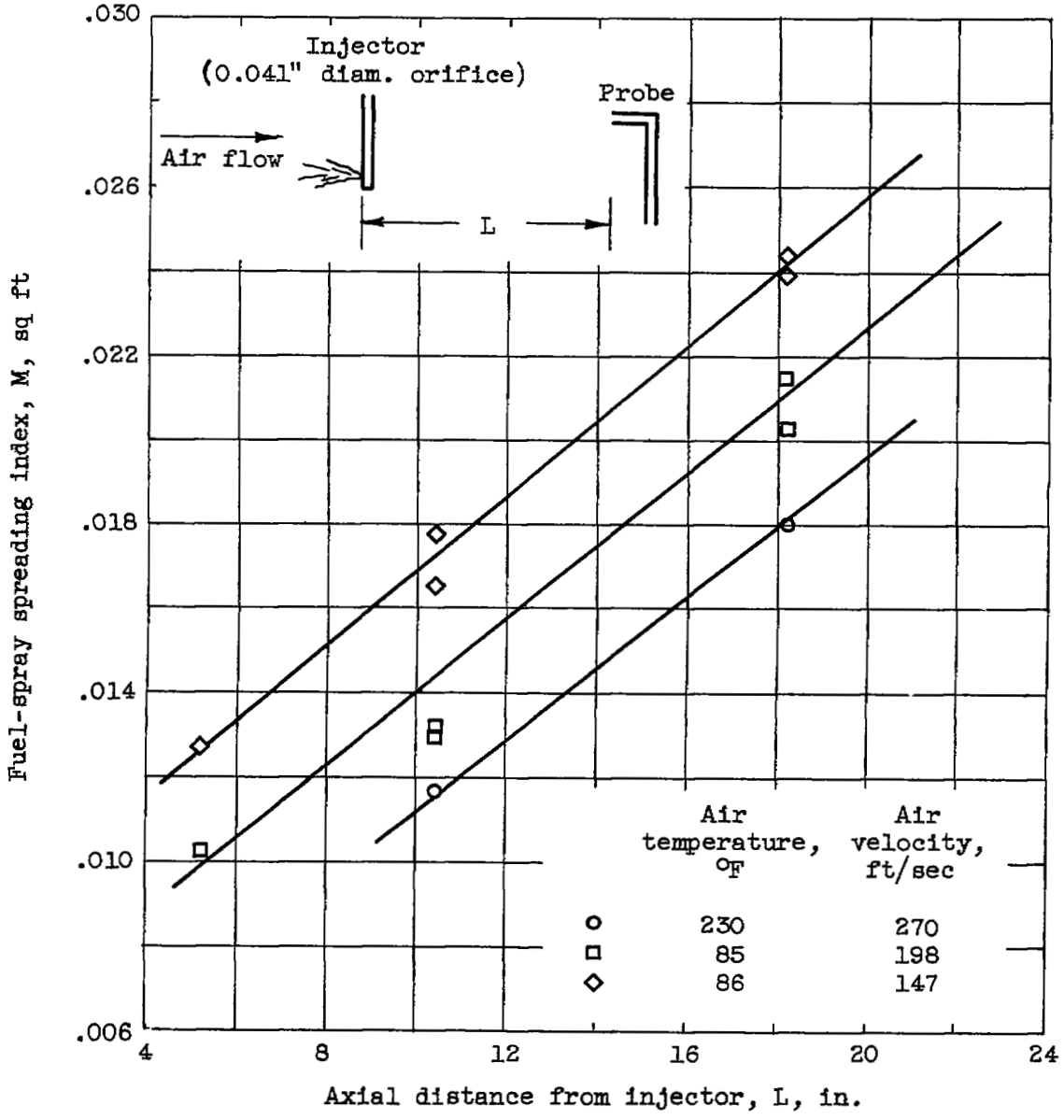

Figure 15. - Effect of sampling distance on fuel-spray spreading index. Fuel, isooctane; air pressure, 25 inches of mercury absolute; fuel-injection pressure drop, 55 pounds per square inch.

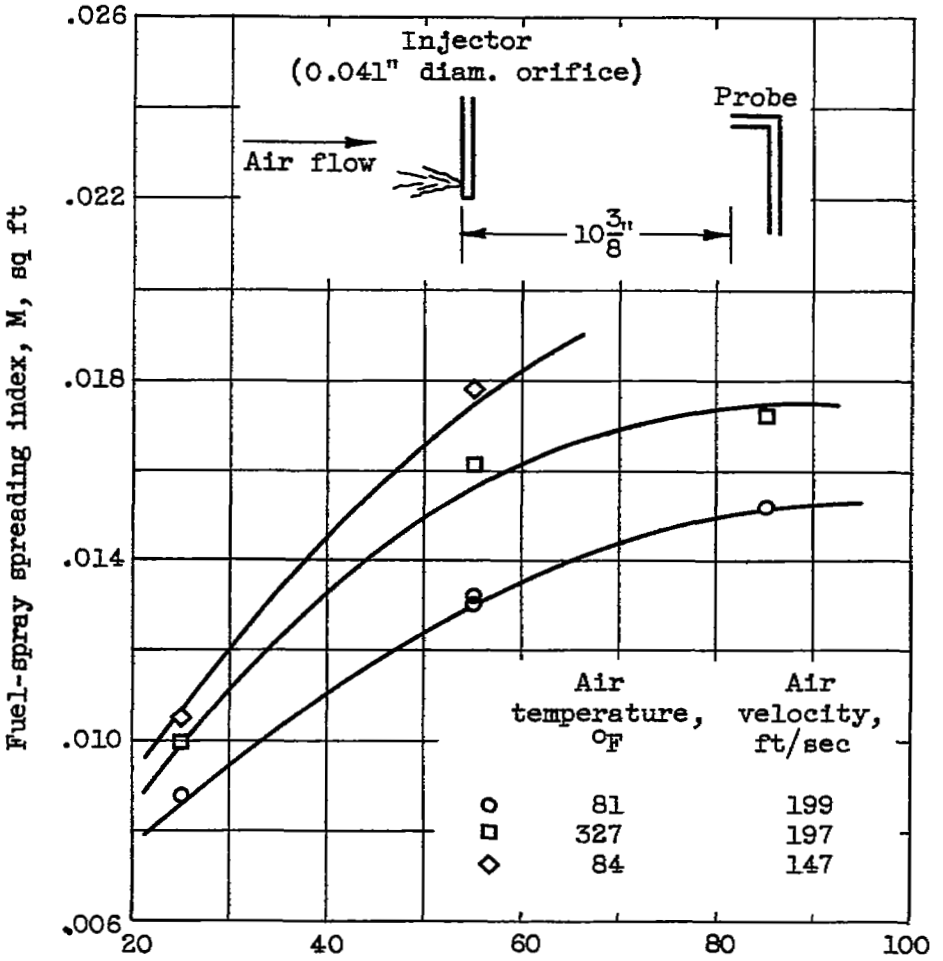

Figure 16. - Effect of fuel-injection pressure drop on fuel-spray spreading index. Fuel, isooctane; air pressure, 25 inches of mercury absolute.

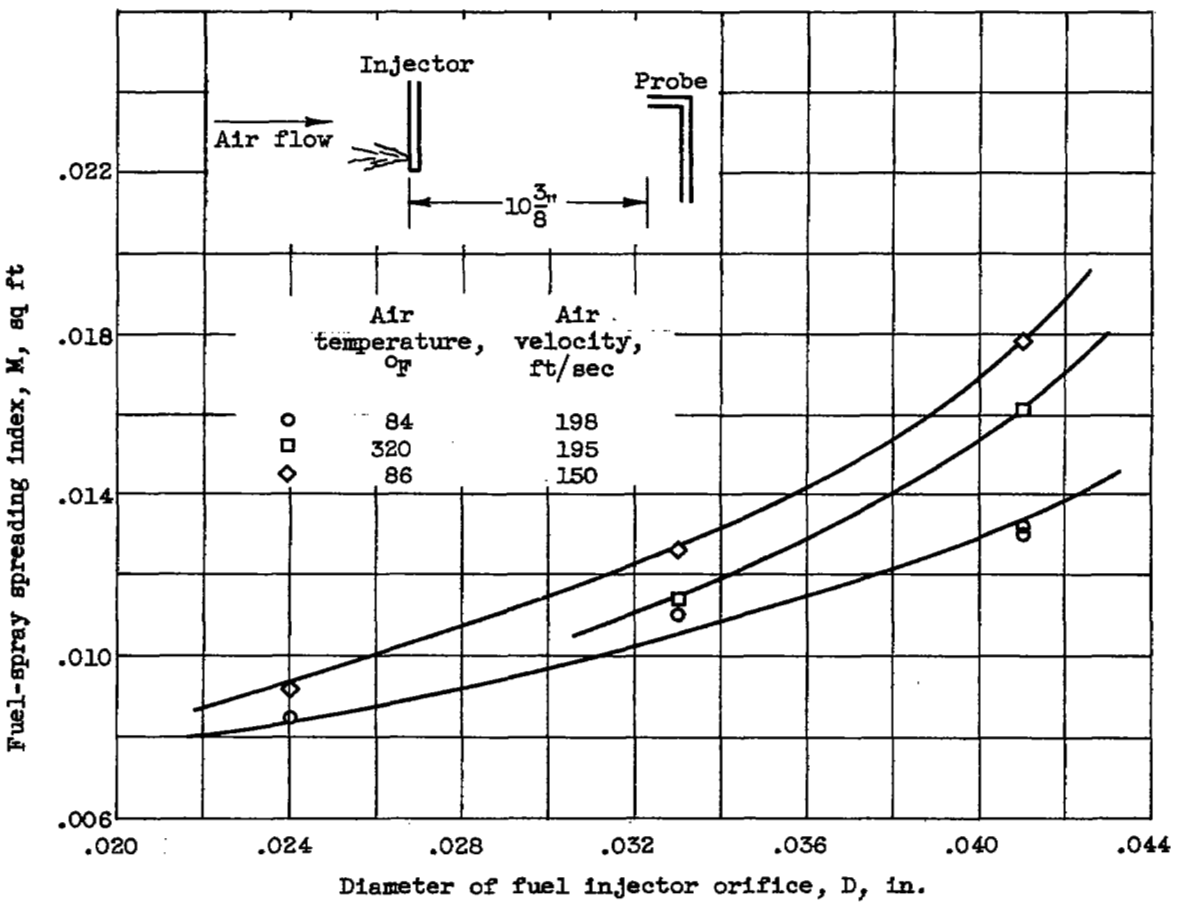

Figure 17. - Effect of orifice size on fuel-spray spreading index. Fuel, isooctane; air pressure, 25 inches of mercury absolute; fuel-injection pressure drop, 55 pounds per square inch.

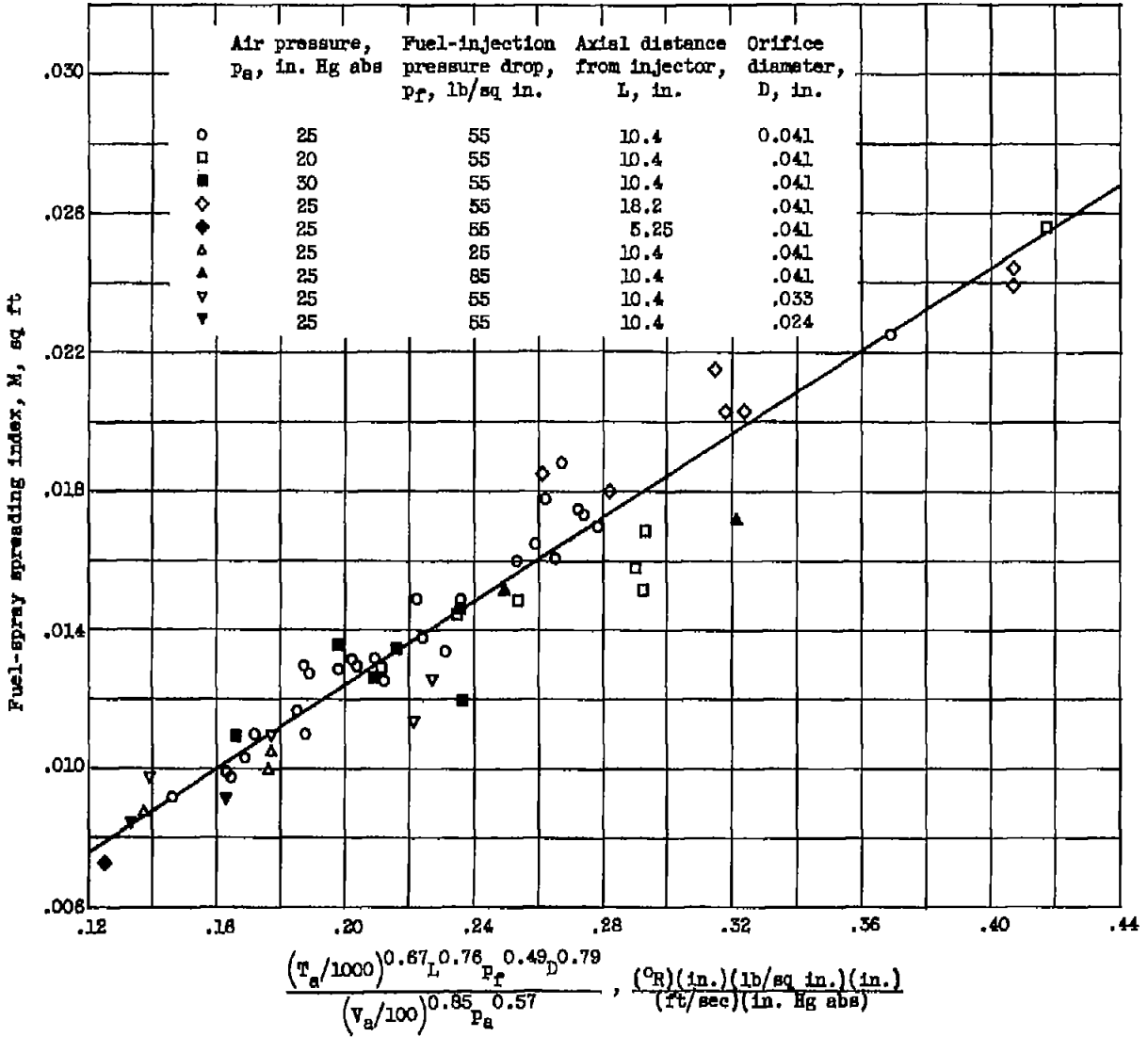

Figure 18. - Correlation of index of fuel-spray spreading. Fuel, isooctane; air velocity, 100 to 350 feet per second; air temperature, 80° to 390° F.